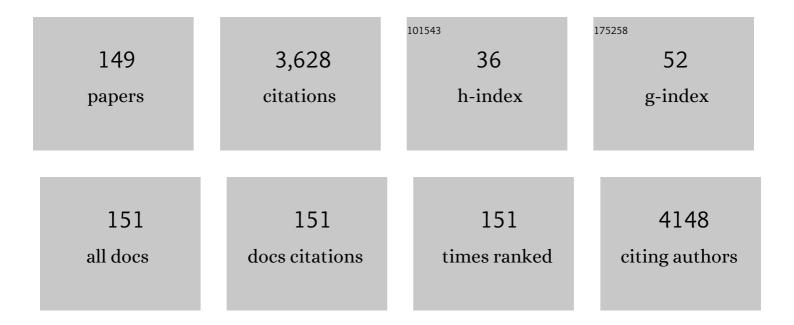
## Wenxian X Li

List of Publications by Year in descending order

Source: https://exaly.com/author-pdf/4543192/publications.pdf Version: 2024-02-01



WENYIAN XII

#	Article	IF	CITATIONS
1	Bifunctional water splitting enhancement by manipulating Mo-H bonding energy of transition Metal-Mo2C heterostructure catalysts. Chemical Engineering Journal, 2022, 431, 134126.	12.7	49
2	U7Co 3d impurity energy level mediated photogenerated carriers transfer in Bi2S3/ZnS:Co/TiO2 photoanode. Chemical Engineering Journal, 2022, 433, 134458.	12.7	8
3	Electrocatalyst nanoarchitectonics with molybdenum-cobalt bimetallic alloy encapsulated in nitrogen-doped carbon for water splitting reaction. Journal of Alloys and Compounds, 2022, 904, 164084.	5.5	29
4	<i>In situ</i> phase transition induced TM–MoC/Mo <sub>2</sub> C (TM= Fe, Co, Ni, and Cu) heterostructure catalysts for efficient hydrogen evolution. Journal of Materials Chemistry A, 2022, 10, 10493-10502.	10.3	20
5	Carbon-based bifunctional electrocatalysts for oxygen reduction and oxygen evolution reactions: Optimization strategies and mechanistic analysis. Journal of Energy Chemistry, 2022, 71, 234-265.	12.9	78
6	The effect of coordination environment on the activity and selectivity of single-atom catalysts. Coordination Chemistry Reviews, 2022, 461, 214493.	18.8	91
7	Metal-organic frameworks-derived nitrogen-doped carbon with anchored dual-phased phosphides as efficient electrocatalyst for overall water splitting. Sustainable Materials and Technologies, 2022, 32, e00421.	3.3	6
8	Mo-induced in-situ architecture of NixCoyP/Co2P heterostructure nano-networks on nickel foam as bifunctional electrocatalysts for overall water splitting. Sustainable Materials and Technologies, 2022, 33, e00461.	3.3	11
9	Urchin-like cobalt hydroxide coupled with N-doped carbon dots hybrid for enhanced electrocatalytic water oxidation. Chemical Engineering Journal, 2021, 420, 127598.	12.7	29
10	Enhanced photoelectrochemical water-splitting performance with a hierarchical heterostructure: Co3O4 nanodots anchored TiO2@P-C3N4 core-shell nanorod arrays. Chemical Engineering Journal, 2021, 404, 126458.	12.7	56
11	Progress on modification of microstructures and magnetic properties of Nd-Fe-B magnets by the grain boundary diffusion engineering. Journal of Magnetism and Magnetic Materials, 2021, 517, 167278.	2.3	25
12	FeS2 bridging function to enhance charge transfer between MoS2 and g–C3N4 for efficient hydrogen evolution reaction. Chemical Engineering Journal, 2021, 421, 127804.	12.7	51
13	Coercivity enhancement in Dy-free HDDR Nd-Fe-B powders by the grain boundary diffusion of Zn. Journal of Magnetism and Magnetic Materials, 2021, 523, 167589.	2.3	4
14	Interfacial Charge Transport in 1D TiO <sub>2</sub> Based Photoelectrodes for Photoelectrochemical Water Splitting. Small, 2021, 17, e1903378.	10.0	102
15	Surface and Interface Engineering: Molybdenum Carbide–Based Nanomaterials for Electrochemical Energy Conversion. Small, 2021, 17, e1903380.	10.0	87
16	Cobalt Chalcogenides/Cobalt Phosphides/Cobaltates with Hierarchical Nanostructures for Anode Materials of Lithiumâ€lon Batteries: Improving the Lithiation Environment. Small, 2021, 17, e1903418.	10.0	30
17	Integrating nonâ€ŧargeted metabolomics and toxicology networks to study the mechanism of Esculentoside Aâ€induced hepatotoxicity in rats. Journal of Biochemical and Molecular Toxicology, 2021, 35, 1-15.	3.0	11
18	Facile Fabrication of Hybrid Perovskite Singleâ€Crystalline Photocathode for Photoelectrochemical Water Splitting. Energy Technology, 2021, 9, 2000965.	3.8	6

#	Article	IF	CITATIONS
19	Improved electrochemical performances of LiNi0.5Co0.2Mn0.3O2 modified by Graphene/V2O5 co-coating. Ceramics International, 2021, 47, 21759-21768.	4.8	12
20	Enhancement of the electrochemical performances for LiNi0.6Co0.2Mn0.2O2 at high cut-off voltage by an effective dual-coating. Ionics, 2021, 27, 3239-3249.	2.4	3
21	Coating ultra-thin TiN layer onto LiNi0.8Co0.1Mn0.1O2 cathode material by atomic layer deposition for high-performance lithium-ion batteries. Journal of Alloys and Compounds, 2021, 888, 161594.	5.5	20
22	Porous Mn-doped cobalt phosphide nanosheets as highly active electrocatalysts for oxygen evolution reaction. Chemical Engineering Journal, 2021, 425, 131642.	12.7	71
23	Hierarchical molybdenum phosphide coupled with carbon as a whole pH-range electrocatalyst for hydrogen evolution reaction. Applied Catalysis B: Environmental, 2020, 260, 118196.	20.2	142
24	Concrete-like high sulfur content cathodes with enhanced electrochemical performance for lithium-sulfur batteries. Journal of Energy Chemistry, 2020, 42, 174-179.	12.9	16
25	Recent progress in thermal/environmental barrier coatings and their corrosion resistance. Rare Metals, 2020, 39, 498-512.	7.1	58
26	Anti-perovskite carbides and nitrides A3BX: A new family of damage tolerant ceramics. Journal of Materials Science and Technology, 2020, 40, 64-71.	10.7	15
27	Modification of LiNi0.5Co0.2Mn0.3O2 with a NaAlO2 coating produces a cathode with increased long-term cycling performance at a high voltage cutoff. Ceramics International, 2020, 46, 7625-7633.	4.8	19
28	3D freestanding flower-like nickel-cobalt layered double hydroxides enriched with oxygen vacancies as efficient electrocatalysts for water oxidation. Sustainable Materials and Technologies, 2020, 25, e00170.	3.3	8
29	Bridging metal-ion induced vertical growth of MoS2 and overall fast electron transfer in (C,P)3N4-M (Ni2+, Co2+)-MoS2 electrocatalyst for efficient hydrogen evolution reaction. Sustainable Materials and Technologies, 2020, 25, e00172.	3.3	7
30	High temperature mechanical and thermal properties of CaxBa1-xZrO3 solid solutions. Ceramics International, 2020, 46, 17416-17422.	4.8	5
31	Zinc interstitial and oxygen vacancy mediated high Curie-temperature ferromagnetism in Ag-doped ZnO. Ceramics International, 2020, 46, 18639-18647.	4.8	25
32	Donor-acceptor codoping effects on tuned visible light response of TiO2. Journal of Environmental Chemical Engineering, 2020, 8, 104168.	6.7	12
33	Functionalised hexagonal boron nitride for energy conversion and storage. Journal of Materials Chemistry A, 2020, 8, 14384-14399.	10.3	96
34	Atomic layer deposition for improved lithiophilicity and solid electrolyte interface stability during lithium plating. Energy Storage Materials, 2020, 28, 17-26.	18.0	47
35	Carbon-Coating Layers on Boron Generated High Critical Current Density in MgB2 Superconductor. ACS Applied Materials & Interfaces, 2020, 12, 8563-8572.	8.0	10
36	Single-layered GO/LDH hybrid nanoporous membranes with improved stability for salt and organic molecules rejection. Journal of Membrane Science, 2020, 607, 118184.	8.2	30

#	Article	IF	CITATIONS
37	Research Progress of Electromagnetic Properties of MgB2 Induced by Carbon-Containing Materials Addition and Process Techniques. Acta Metallurgica Sinica (English Letters), 2020, 33, 471-489.	2.9	6
38	Uniform Li Deposition Sites Provided by Atomic Layer Deposition for the Dendrite-free Lithium Metal Anode. ACS Applied Materials & Interfaces, 2020, 12, 19530-19538.	8.0	30
39	Al-doped ZnO (AZO) modified LiNi0.8Co0.1Mn0.1O2 and their performance as cathode material for lithium ion batteries. Materials Chemistry and Physics, 2020, 251, 123085.	4.0	24
40	Nanomagnetism variation with fluorine content in Co(OH)F. Journal of Alloys and Compounds, 2020, 825, 153916.	5.5	5
41	Improvement in the cycling stability and rate capability of LiNi0.5Co0.2Mn0.3O2 cathode material via the use of a Ta2O5 coating. Ceramics International, 2020, 46, 14931-14939.	4.8	18
42	Magnetic Responsive MnO2 Nanomaterials. Springer Series in Materials Science, 2020, , 139-163.	0.6	0
43	Rare earth doping effects on superconducting properties of MgB2: AÂreview. Journal of Rare Earths, 2019, 37, 124-133.	4.8	21
44	Bifunctional iron nickel phosphide nanocatalysts supported on porous carbon for highly efficient overall water splitting. Sustainable Materials and Technologies, 2019, 22, e00117.	3.3	21
45	Study on the high magnetic field processed ZnO based diluted magnetic semiconductors. Ceramics International, 2019, 45, 19583-19595.	4.8	17
46	Artificial 2D Flux Pinning Centers in MgB2 Induced by Graphitic-Carbon Nitride Coated on Boron for Superconductor Applications. ACS Applied Nano Materials, 2019, 2, 5399-5408.	5.0	6
47	Microstructure and property evolution of diamond-like carbon films co-doped by Al and Ti with different ratios. Surface and Coatings Technology, 2019, 361, 83-90.	4.8	31
48	Room Temperature Ferromagnetism Enhanced in Alâ€Đoped ZnO by Pulsed Magnetic Field Processing. Crystal Research and Technology, 2019, 54, 1800223.	1.3	1
49	Metal-ion bridged high conductive RGO-M-MoS2 (M = Fe3+, Co2+, Ni2+, Cu2+ and Zn2+) composite electrocatalysts for photo-assisted hydrogen evolution. Applied Catalysis B: Environmental, 2019, 246, 129-139.	20.2	63
50	Cobalt Oxide Supported on Phosphorus-Doped g-C <sub>3</sub> N <sub>4</sub> as an Efficient Electrocatalyst for Oxygen Evolution Reaction. ACS Applied Energy Materials, 2019, 2, 4718-4729.	5.1	62
51	Cobalt porphyrin (CoTCPP) advanced visible light response of g-C3N4 nanosheets. Sustainable Materials and Technologies, 2019, 22, e00114.	3.3	9
52	Beyond Seashells: Bioinspired 2D Photonic and Photoelectronic Devices. Advanced Functional Materials, 2019, 29, 1901460.	14.9	78
53	Structural, ferromagnetic, and optical properties of Fe and Al co-doped ZnO diluted magnetic semiconductor nanoparticles synthesized under high magnetic field. Advances in Manufacturing, 2019, 7, 248-255.	6.1	10
54	Recent advances in high energy-density cathode materials for sodium-ion batteries. Sustainable Materials and Technologies, 2019, 21, e00098.	3.3	43

#	Article	IF	CITATIONS
55	Enhancement of ferromagnetic properties in (Fe, Ni) co-doped ZnO flowers by pulsed magnetic field processing. Journal of Materials Science: Materials in Electronics, 2019, 30, 8226.	2.2	4
56	Extrinsic Two-Dimensional Flux Pinning Centers in MgB <sub>2</sub> Superconductors Induced by Graphene-Coated Boron. ACS Applied Materials & Interfaces, 2019, 11, 10818-10828.	8.0	18
57	LiFePO4/(C+Cu) composite with excellent cycling stability as lithium ion battery cathodes synthesized via a modified carbothermal reduction method. Ceramics International, 2018, 44, 12106-12111.	4.8	12
58	Crystal Facet Effects on Nanomagnetism of Co <sub>3</sub> O <sub>4</sub> . ACS Applied Materials & Interfaces, 2018, 10, 19235-19247.	8.0	47
59	Accordion-like nanoporous carbon derived from Al-MOF as advanced anode material for sodium ion batteries. Microporous and Mesoporous Materials, 2018, 270, 67-74.	4.4	22
60	Ferromagnetic coupling of Fe3+-VO-Fe3+polarons in Fe-doped ZnO. Ceramics International, 2018, 44, 71-75.	4.8	13
61	Magnetic coupling in Mn <sub>3</sub> O <sub>4</sub> -coated γ-MnOOH nanowires. Surface Innovations, 2018, 6, 250-257.	2.3	3
62	Oxygen vacancy induced ferromagnetism in Cu-doped ZnO. Ceramics International, 2017, 43, 3166-3170.	4.8	75
63	Solvothermal Synthesis of a Hollow Micro-Sphere LiFePO4/C Composite with a Porous Interior Structure as a Cathode Material for Lithium Ion Batteries. Nanomaterials, 2017, 7, 368.	4.1	11
64	Magnetic Characterization of Nanodendritic Platinum. , 2017, , 431-456.		0
65	A facile synthesis of core-shell structured ZnO@C nanosphere and their high performance for lithium ion battery anode. Materials Letters, 2016, 171, 244-247.	2.6	36
66	LiFePO4/C nanocomposite synthesized by a novel carbothermal reduction method and its electrochemical performance. Ceramics International, 2016, 42, 11422-11428.	4.8	20
67	Photocatalytic properties of TiO 2 : Effect of niobium and oxygen activity on partial water oxidation. Applied Catalysis B: Environmental, 2016, 198, 243-253.	20.2	37
68	Manipulating coupling state and magnetism of Mn-doped ZnO nanocrystals by changing the coordination environment of Mn via hydrogen annealing. Chinese Physics B, 2016, 25, 017301.	1.4	4
69	Effect of oxygen vacancy induced by pulsed magnetic field on the room-temperature ferromagnetic Ni-doped ZnO synthesized by hydrothermal method. Journal of Alloys and Compounds, 2016, 675, 286-291.	5.5	44
70	High Critical Current Density MgB2. , 2015, , .		1
71	Fish-scale bio-inspired multifunctional ZnO nanostructures. NPG Asia Materials, 2015, 7, e232-e232.	7.9	56
72	Photocatalytic Properties of TiO <sub>2</sub> : Evidence of the Key Role of Surface Active Sites in Water Oxidation. Journal of Physical Chemistry A, 2015, 119, 9465-9473.	2.5	44

#	Article	IF	CITATIONS
73	Underwater Self-Cleaning Scaly Fabric Membrane for Oily Water Separation. ACS Applied Materials & Interfaces, 2015, 7, 4336-4343.	8.0	113
74	Microscopic unravelling of nano-carbon doping in MgB2 superconductors fabricated by diffusion method. Journal of Alloys and Compounds, 2015, 644, 900-905.	5.5	17
75	Nano-sized LiFePO4/C composite with core-shell structure as cathode material for lithium ion battery. Electrochimica Acta, 2015, 176, 689-693.	5.2	38
76	Enhancement of zinc vacancies in room-temperature ferromagnetic Cr–Mn codoped ZnO nanorods synthesized by hydrothermal method under high pulsed magnetic field. Journal of Alloys and Compounds, 2015, 647, 823-829.	5.5	21
77	Visible-Light Photocatalytic Activity of S-Doped α-Bi <sub>2</sub> O <sub>3</sub> . Journal of Physical Chemistry C, 2015, 119, 14094-14101.	3.1	56
78	Characterisation of nano-grains in MgB2 superconductors by transmission Kikuchi diffraction. Scripta Materialia, 2015, 101, 36-39.	5.2	15
79	Effect of oxygen activity on semiconducting properties of TiO2 (rutile). Ionics, 2015, 21, 1399-1406.	2.4	5
80	Performance modulation of α-MnO2 nanowires by crystal facet engineering. Scientific Reports, 2015, 5, 8987.	3.3	88
81	Transition metal-doped ZnO diluted magnetic semiconductors tuned by high pulsed magnetic field. , 2015, , .		0
82	Rapid microwave-assisted synthesis of various MnO2 nanostructures and their magnetic properties. Materials Chemistry and Physics, 2015, 166, 42-48.	4.0	13
83	Enhancement of critical current of SiC and malic acid codoped MgB2â^•Fe wires. International Journal of Modern Physics B, 2015, 29, 1542032.	2.0	5
84	Influence of electronic structures of doped TiO <sub>2</sub> on their photocatalysis. Physica Status Solidi - Rapid Research Letters, 2015, 9, 10-27.	2.4	49
85	A Time Series Observation of Chinese Children Undergoing Rigid Bronchoscopy for an Inhaled Foreign Body. Chinese Medical Journal, 2015, 128, 504-509.	2.3	22
86	Configuration-induced vortex motion in type-II superconducting films with periodic magnetic dot arrays. Superconductor Science and Technology, 2014, 27, 065004.	3.5	2
87	Phototunable Underwater Oil Adhesion of Micro/Nanoscale Hierarchicalâ€Structured ZnO Mesh Films with Switchable Contact Mode. Advanced Functional Materials, 2014, 24, 536-542.	14.9	67
88	Concentration of electrons at grain boundaries in TiO2 (rutile): Impact on charge transport and reactivity. Catalysis Today, 2014, 224, 200-208.	4.4	12
89	Patterned liquid permeation through the TiO2 nanotube array coated Ti mesh by photoelectric cooperation for liquid printing. Journal of Materials Chemistry A, 2014, 2, 2498.	10.3	8
90	On the roles of graphene oxide doping for enhanced supercurrent in MgB <sub>2</sub> based superconductors. Nanoscale, 2014, 6, 6166-6172.	5.6	40

#	Article	IF	CITATIONS
91	Photoelectric cooperative patterning of liquid permeation on the micro/nano hierarchically structured mesh film with low adhesion. Nanoscale, 2014, 6, 12822-12827.	5.6	27
92	Platinum dendritic nanoparticles with magnetic behavior. Journal of Applied Physics, 2014, 116, .	2.5	18
93	Uncoupled surface spin induced exchange bias in α-MnO2 nanowires. Scientific Reports, 2014, 4, 6641.	3.3	39
94	Graphene Micro-Substrate Induced High Electron-Phonon Coupling in \$hbox{MgB}_{2}\$. IEEE Transactions on Applied Superconductivity, 2013, 23, 7000104-7000104.	1.7	16
95	The variation of Mn-dopant distribution state with x and its effect on the magnetic coupling mechanism in Zn 1â^' x Mn x O nanocrystals. Chinese Physics B, 2013, 22, 107501.	1.4	4
96	Effect of Sintering Temperature on the Superconducting Properties of Graphene Doped \$hbox{MgB}_{2}\$. IEEE Transactions on Applied Superconductivity, 2013, 23, 7100604-7100604.	1.7	19
97	A significant improvement in both low- and high-field performance of MgB2 superconductors through graphene oxide doping. Scripta Materialia, 2013, 69, 437-440.	5.2	22
98	Magnetotransport dependence on the field magnitude and direction in large area epitaxial graphene film on stretchable substrates. Applied Physics Letters, 2013, 102, .	3.3	4
99	Enhancing the Superconducting Properties of Magnesium Diboride Without Doping. Journal of the American Ceramic Society, 2013, 96, 2893-2897.	3.8	5
100	Dependence of magnetoelectric properties on sintering temperature for nano-SiC-doped MgB2/Fe wires made by combined in situ/ex situ process. Journal of Applied Physics, 2012, 111, 07E135.	2.5	11
101	Magnetic and superconducting properties of spin-fluctuation-limited superconducting nanoscale VNx. Journal of Applied Physics, 2012, 111, .	2.5	0
102	The Effects of Graphene Doping on the In-Field <i>J<sub>c</sub></i> of MgB <sub>2</sub> Wires. Journal of Nanoscience and Nanotechnology, 2012, 12, 1402-1405.	0.9	6
103	Chemically induced electric field: flat band potential engineering. , 2012, , .		0
104	The effect of reduced graphene oxide addition on the superconductivity of MgB2. Journal of Materials Chemistry, 2012, 22, 13941.	6.7	43
105	Structural control of d-f interaction in the CeFe <sub>1â^'x</sub> Ru <sub>x</sub> AsO system. Europhysics Letters, 2012, 99, 57009.	2.0	8
106	Magnetoelectric properties of MgB <inf>2</inf> superconductor by SiC doping. , 2011, , .		0
107	Graphene–V2O5•nH2O xerogel composite cathodes for lithium ion batteries. RSC Advances, 2011, 1, 690.	3.6	84
108	Effect of thermal strain on <i>Jc</i> and <i>Tc</i> in high density nano-SiC doped MgB2. Journal of Applied Physics, 2011, 109, .	2.5	11

#	Article	IF	CITATIONS
109	Evaluation of carbon incorporation and strain of doped MgB2 superconductor by Raman spectroscopy. Scripta Materialia, 2011, 64, 323-326.	5.2	9
110	Flux pinning mechanisms in graphene-doped MgB2 superconductors. Scripta Materialia, 2011, 65, 634-637.	5.2	39
111	Graphene micro-substrate-induced π gap expansion in MgB2. Acta Materialia, 2011, 59, 7268-7276. Direct Observation of Local Potassium Variation and Its Correlation to Electronic Inhomogeneity	7.9	17
112	in <mml:math display="inline" xmlns:mml="http://www.w3.org/1998/Math/MathML"><mml:mo´ stretchy="false"&gt;(<mml:msub><mml:mi>Ba</mml:mi><mml:mrow><mml:mn>1</mml:mn><mml:m< td=""><td>⊃&gt;â^'∢/mn 7.8</td><td>nl:mo&gt; &lt; mml:m 48</td></mml:m<></mml:mrow></mml:msub></mml:mo´ </mml:math>	⊃>â^'∢/mn 7.8	nl:mo> < mml:m 48
113	Physical Review Letters, 2011, 106, 247002. Improving Superconducting Properties of MgB\$_{2}\$ by Graphene Doping. IEEE Transactions on Applied Superconductivity, 2011, 21, 2686-2689.	1.7	26
114	The effects of size and orientation on magnetic properties and exchange bias in Co3O4 mesoporous nanowires. Journal of Applied Physics, 2011, 109, .	2.5	18
115	Evolution of Electromagnetic Properties and Microstructure With Sintering Temperature for \${hbox {MgB}}_{2}{hbox {Fe}} Wires Made by Combined In-Situ/Ex-Situ Process. IEEE Transactions on Applied Superconductivity, 2011, 21, 2635-2638.	1.7	8
116	Raman Spectroscopy: Alternate Method for Strain and Carbon Substitution Study in \${m MgB}_{2}\$. IEEE Transactions on Applied Superconductivity, 2011, 21, 2623-2626.	1.7	1
117	Prevalence and clinical significance of 15 autoantibodies in patients with new-onset systemic lupus erythematosus. Irish Journal of Medical Science, 2010, 179, 623-627.	1.5	3
118	Dependence of superconducting properties on lattice strain in MgB2. Physica C: Superconductivity and Its Applications, 2010, 470, S629-S630.	1.2	3
119	Effects of ball-mill processing on the superconductivity of sucrose doped MgB2. Physica C: Superconductivity and Its Applications, 2010, 470, S710-S711.	1.2	3
120	The mechanism of Tc performance for Zn doped MgB2 sintered in magnetic field. Physica C: Superconductivity and Its Applications, 2010, 470, S644-S645.	1.2	1
121	Synthesis and characteristics of MgB2 bulks with different densities. Physica C: Superconductivity and Its Applications, 2010, 470, S669-S670.	1.2	5
122	Stress evolution and lattice distortion induced by thickness variation and lattice misfit in La0.67Sr0.33MnO3â~δ films. Solid State Communications, 2010, 150, 66-69.	1.9	11
123	(00l)-oriented Bi2Sr2Co2Oy and Ca3Co4O9 films: Self-assembly orientation and growth mechanism by chemical solution deposition. Acta Materialia, 2010, 58, 4281-4291.	7.9	47
124	Effect of Mg/B ratio on the superconductivity of <mml:math xmlns:mml="http://www.w3.org/1998/Math/MathML" display="inline"&gt;<mml:mrow><mml:msub><mml:mrow><mml:mtext>MgB</mml:mtext></mml:mrow><mml:mu with SiC addition. Physical Review B, 2010, 81, .</mml:mu </mml:msub></mml:mrow></mml:math 	ı>2∛7mml	:m10 :mn>
125	Magnetic scattering effects in two-band superconductor: the ferromagnetic dopants in MgB <sub>2</sub> . Journal of Physics Condensed Matter, 2010, 22, 135701.	1.8	10
126	Three first order magnetic phase transitions in re-entrant ferromagnet PrMn1.4Fe0.6Ge2. Journal of Alloys and Compounds, 2010, 505, L38-L42.	5.5	6

#	Article	IF	CITATIONS
127	Magnetic properties and magnetocaloric effect of (Mn1-xNix)3Sn2(x=0–0.5) compounds. Journal of Applied Physics, 2009, 105, .	2.5	9
128	T <sub>C</sub> ENHANCEMENT FOR NANO- <font>SiC</font> DOPED <font>MgB</font> <sub>2</sub> SUPERCONDUCTORS SINTERED IN 5T PULSED MAGNETIC FIELD. International Journal of Modern Physics B, 2009, 23, 3482-3485.	2.0	2
129	HIGH CRITICAL CURRENT DENSITY OF <font>MgB</font> <sub>2</sub> BULKS SINTERED IN FLOWING WELDING GRADE <font>Ar</font> ATMOSPHERE. International Journal of Modern Physics B, 2009, 23, 3538-3541.	2.0	1
130	The combined influence of connectivity and disorder on Jc and Tc performances in MgxB2+10wt %SiC. Journal of Applied Physics, 2009, 106, 093906.	2.5	16
131	Improved superconducting properties of in situ powder-in-tube processed wires with nano-size SiC addition. Physica C: Superconductivity and Its Applications, 2009, 469, 1519-1522.	1.2	6
132	Synthesis, crystal structure and magnetic properties of a cyanide-bridged FellI–MnIII bimetallic chain based on [Fe(bipy)(CN)4]â^' building block. Journal of Molecular Structure, 2009, 921, 341-345.	3.6	6
133	Thermal-strain-induced enhancement of electromagnetic properties of SiC–MgB2 composites. Applied Physics Letters, 2009, 94, 042510.	3.3	40
134	Increased Superconductivity for CNT Doped \${hbox {MgB}}_{2}\$ Sintered in 5T Pulsed Magnetic Field. IEEE Transactions on Applied Superconductivity, 2009, 19, 2752-2755.	1.7	3
135	Stress/Strain Induced Flux Pinning in Highly Dense \${m MgB}_{2}\$ Bulks. IEEE Transactions on Applied Superconductivity, 2009, 19, 2722-2725.	1.7	6
136	Optimization of Nominal Mixing Ratio of Mg to B in Fabrication of Magnesium Diboride Bulk. IEEE Transactions on Applied Superconductivity, 2009, 19, 2775-2779.	1.7	1
137	HYDROTHERMAL SYNTHESIS OF <font>ZnO</font> NANOSTRUCTURES UNDER HIGH PULSED MAGNETIC FIELD. International Journal of Modern Physics B, 2009, 23, 3655-3659.	2.0	6
138	Electron–phonon coupling properties in MgB <sub>2</sub> observed by Raman scattering. Journal of Physics Condensed Matter, 2008, 20, 255235.	1.8	23
139	Raman study of element doping effects on the superconductivity of <mml:math xmlns:mml="http://www.w3.org/1998/Math/MathML" display="inline"&gt; <mml:mrow> <mml:msub> <mml:mi> MgB </mml:mi> <mml:mn> 2 </mml:mn> </mml:msub> Physical Review B, 2008, 77</mml:mrow></mml:math 	ıl:m²o²w><,	/mml:math>
140	Excess Mg addition MgB2/Fe wires with enhanced critical current density. Journal of Applied Physics, 2008, 103, 083911.	2.5	16
141	Raman study on the effects of sintering temperature on the Jc(H) performance of MgB2 superconductor. Journal of Applied Physics, 2008, 103, 013511.	2.5	20
142	Improvement of <i>J</i> <sub>c</sub> and <i>H</i> <sub>c2</sub> in MgB <sub>2</sub> superconductor with citric acid addition. Journal of Physics: Conference Series, 2008, 97, 012215.	0.4	1
143	Significant improvement in the critical current density of <i>in situ</i> MgB <sub>2</sub> by excess Mg addition. Superconductor Science and Technology, 2007, 20, L43-L47.	3.5	34
144	Benzoic Acid Doping to Enhance Electromagnetic Properties of \${m MgB}_{2}\$ Superconductors. IEEE Transactions on Applied Superconductivity, 2007, 17, 2778-2781.	1.7	9

#	Article	IF	CITATIONS
145	Effect of magnetic field processing on the microstructure of micronsize Zn doped MgB2. Physica C: Superconductivity and Its Applications, 2007, 460-462, 310-311.	1.2	5
146	Effect of magnetic field processing on the microstructure of carbon nanotubes doped MgB2. Physica C: Superconductivity and Its Applications, 2007, 460-462, 570-571.	1.2	13
147	Magnetic field processing to enhance critical current densities of MgB2 superconductors. Applied Physics Letters, 2006, 89, 202504.	3.3	25
148	Superconducting Properties of Carbonaceous Chemical Doped MgB2. , 0, , .		3
149	Magnetic Ground State and Tunable Néel Temperature in the Spin ½ Linear Chain Antiferromagnet Co(OH) (2â~' x ) F x. Physica Status Solidi (B): Basic Research, 0, , 2100438.	1.5	1